

---

Retrospective Theses and Dissertations

---

Spring 1982

## A Dynamic Analysis of an Explosion Driven Hydrodynamic Conical Distributed Breach Shock Tube

Lee E. Griesemer  
*University of Central Florida*

 Part of the [Engineering Commons](#)

Find similar works at: <https://stars.library.ucf.edu/rtd>

University of Central Florida Libraries <http://library.ucf.edu>

This Masters Thesis (Open Access) is brought to you for free and open access by STARS. It has been accepted for inclusion in Retrospective Theses and Dissertations by an authorized administrator of STARS. For more information, please contact [STARS@ucf.edu](mailto:STARS@ucf.edu).

---

### STARS Citation

Griesemer, Lee E., "A Dynamic Analysis of an Explosion Driven Hydrodynamic Conical Distributed Breach Shock Tube" (1982). *Retrospective Theses and Dissertations*. 627.  
<https://stars.library.ucf.edu/rtd/627>

A DYNAMIC ANALYSIS OF AN EXPLOSION  
DRIVEN HYDRODYNAMIC CONICAL  
DISTRIBUTED BREACH SHOCK TUBE

BY

LEE ERIC GRIESEMER  
B.S.E., University of Central Florida, 1980

RESEARCH REPORT

Submitted in partial fulfillment of the requirements  
for the degree of Master of Science in Engineering  
in the Graduate Studies Program of the  
College of Engineering  
University of Central Florida  
Orlando, Florida

Spring Term  
1982

## ABSTRACT

In order to better simulate an explosive underwater environment, a new design of the existing explosion driven hydrodynamic conical shock tube has been proposed. This new concept calls for the removal of part of the old tube to accomodate a distributed breach plug. The distributed breach should enhance shock wave characteristics by minimizing the energy losses associated with plastic deformations which occur at detonation.

This report makes use of a finite element program, SAP IV, to investigate the modal characteristics of the new distributed breach design. A dynamic response history analysis has also been performed in order to predict the response of the structure to loads characteristic of an ideal shock wave as it propagates along the tube axis. From these efforts some insight has been gained into the structural feasibility of the new design.

## ACKNOWLEDGEMENTS

The author wishes to thank Dr. Sayed M. Metwalli for the guidance which was provided throughout this research effort.

## TABLE OF CONTENTS

LIST OF FIGURES . . . . .	v
Chapter	
I. LITERATURE SEARCH . . . . .	1
II. A NEW DESIGN: THE DISTRIBUTED BREACH . . .	6
III. DYNAMIC ANALYSIS . . . . .	9
Modal Analysis: Pipe Element Model . . .	10
Modal Analysis: Axisymmetric Model . . .	12
Response History Analysis . . . . .	17
IV. SAP IV PROGRAM RESULTS . . . . .	19
CONCLUSION . . . . .	40
REFERENCES . . . . .	42



# LIST OF FIGURES

	<u>Page</u>
1. Existing shock tube configuration . . . . .	5
2. Distributed breach shock tube . . . . .	8
3. SAP IV pipe element . . . . .	11
4. Pipe element model . . . . .	13
5. SAP IV axisymmetric element . . . . .	14
6. Axisymmetric element model . . . . .	16
7. First longitudinal mode shape . . . . .	22
8. Second longitudinal mode shape . . . . .	23
9. Third longitudinal mode shape . . . . .	24
10. First transverse mode shape . . . . .	25
11. Second transverse mode shape . . . . .	26
12. Third transverse mode shape . . . . .	27
13. X-rotational mode shapes . . . . .	28
14. Y-rotational mode shapes . . . . .	29
15. Actual waveform and SAP IV input . . . . .	33
16. Output stress convention . . . . .	36
17. Element 4 longitudinal stress response . . . . .	38
18. Element 17 radial stress response . . . . .	39

## I. LITERATURE SEARCH

In order to simulate an explosive underwater environment, an explosion driven hydrodynamic conical shock tube was developed. The initial design and analysis of the existing structure was reported by Connell (1980). An analysis of the structural dynamic characteristics of the existing tube was also carried out by Sanders (1981).

The particular significance to studies of shock waves produced by high explosives is the relatively small quantity of explosive needed in the conical tube to produce shock waves with characteristics corresponding to those from a much larger quantity of explosive detonated in an unlimited or "free" medium (Filler, 1964). This is the fundamental principle behind the conical shock tube. The portion of the wave isolated by the conical tube ideally has all the characteristics of the complete spherical shock wave. An explosive amplification factor, dependent on tube geometry, is used as a performance characteristic. Thus, a small amount of explosive used in a conical shock tube behaves like a much larger amount. A complete derivation and explanation of the amplification factor is presented by Connell (1980).

The existing shock tube configuration is shown in Figure 1 (Sanders, 1981). The tube was constructed from 8.0 inch diameter steel round. An electric discharge machining process was used to form the interior conical surface. The intermediate flange was necessary to aide in the cleaning and placement of the tube. The breach plug and closure head bolt to flanges at the breach and muzzle end, respectively. A fill and drain apparatus was fitted into a 2.0 inch thick annular steel ring and bolted between the muzzle flange and closure head. All of the tube joints are bolted together using a symmetrical pattern of twelve 3/4 inch grade 5 bolts and sealed with o-ring seals. The breach plug houses the explosive charge.

The original shock tube was designed to generate and withstand a shock wave whose characteristics were equivalent to that of a 125 pound spherical charge of TNT up to a range of 11 feet (Connell, 1980). Empirical correlations, or scaling laws, were used to model the shock wave and the explosive characteristics of TNT. These empirical scaling laws are used by acousticians to approximate the Kirkwood-Bethe theory, which remains the generally accepted theory of explosive shock waves. Although they shed little light on the physics of shock wave propagation, these scaling laws, in a practical sense, have been astonishingly successful (Rogers, 1977).

The pressure-time curve for the shock wave, as given



by Rogers (1977), is assumed to be a shock of amplitude  $P_m$  with an exponentially decaying tail. That is,

$$P(R,t) = P_m(R) \exp[-t/\theta]$$

where

$R$  = range from charge center (ft)

$P_m$  = peak pressure developed (psi)

$\theta$  = time constant (microseconds)

For TNT, Arons (1954) has reported the following relations:

$$P_m(R) = (2.16 \times 10^4) (W^{1/3} R)^{1.13}$$

$$\theta = \frac{58 W^{1/3}}{\left( \frac{W^{1/3}}{R} \right)^{0.22}}$$

where

$W$  = charge weight (pounds)

$R$  = range from charge center (ft)

It should be noted that previous tests with the shock tube showed peak pressure values lower than those values predicted from the scaling laws. The shock tube was, however, designed with the aide of the empirical parameters and thus for higher peak pressures. It would then seem conservative to use these theoretical values for further analysis of the shock tube structure itself. This method of approach should therefore give some insight into predicting the behavior of the tube if the "ideal" spherical wave front and corresponding characteristics were actually achieved.

By recording the actual shock wave history and analyzing the data, Sanders (1981) was able to calculate an actual amplification factor and show that peak pressure estimates were slightly lower than the values predicted from the scaling laws. This data was obtained when using an actual charge weight of only about 58% of the weight calculated by Connell (1980) to produce the desired effect of the design specifications. It was thus suggested that the charge weight needed to reach the required test level might cause permanent damage to the shock tube structure. Therefore, a more in depth analysis of the dynamic response of the shock tube when subjected to the original design loads is desirable. A quantitative analysis of this sort can then be used to predict the structural feasibility of the shock tube when subjected to tests at the required level.

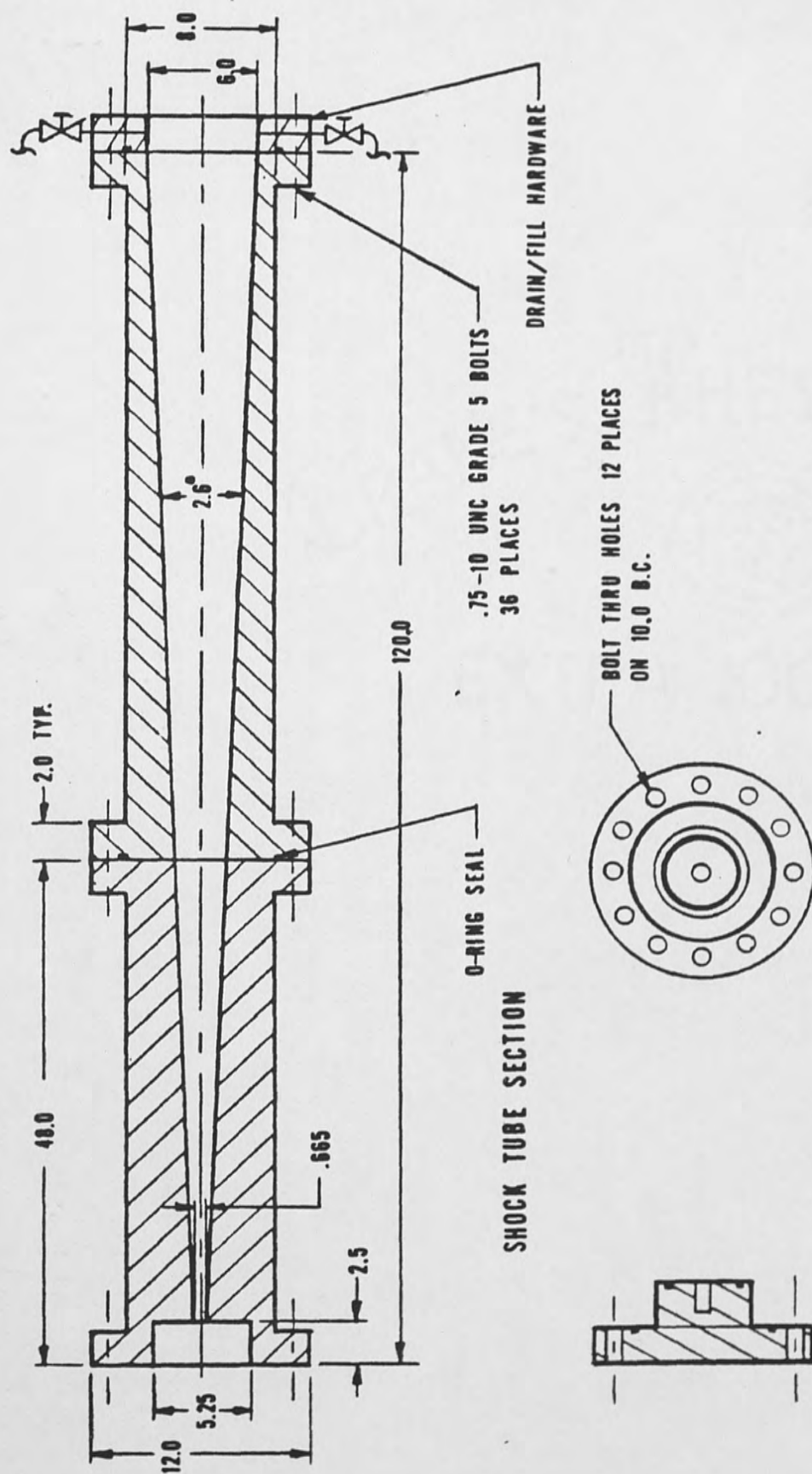


Fig. 1. Existing shock tube configuration

BREACH END PLATE

## II. A NEW DESIGN: THE DISTRIBUTED BREACH

A program of development and redesign of the existing shock tube was proposed by Dr. F. A. Moslehy and Dr. S. M. Metwalli (1982). Successful use of the tube in the past has been limited by plastic deformations in the breach plug resulting from detonation and data noise or "ringing", which occurs after detonation. The plastic deformation in the existing breach plug is an obvious source of energy loss and destruction of the ideal shock front. A possible solution to the plastic deformation problem is to redesign the shock tube so as to accomodate a distributed breach. Minimizing deformations, or energy losses, at the breach should cause wave characteristics and the amplification factor to approach ideal values.

The concept of the new design is that the four foot section of the tube be discarded and an equivalent amount of charge be distributed over a spherical surface at that station. This alteration obviously will cause changes in the structural and dynamic characteristics of the shock tube. It is then desirable to try and predict the dynamic characteristics and dynamic response of the new design.

The distributed breach shock tube design is illustrated in Figure 2. This proposed design will have considerable advantages over the existing design in many ways. The most notable improvement would be to decrease the plastic deformation and associated energy losses at detonation. This is so because around the detonation area the new design provides the existence of a prestressed three dimensional continuum. A triaxial state of stress will then exist and, theoretically, the resistance of the material to loads becomes large. A good explanation and derivation of this theory is given by Timoshenko and Gere (1972) and Shigley (1977). The use of an expendable section and an isolation layer around the breach has been specified in order to prevent damage to the existing shock tube body.

Shock wave characteristics should also be enhanced due to the distribution of the explosive material. It has been hypothesized that the surface of the distributed charge should not be spherical but should actually be concave due to the much greater detonation rate of the charge compared to the propagation rate of the shock wave in water (Moslehy and Metwalli, 1982). A flat surface, however, is to be used to determine the initial feasibility of the design. A more in depth analysis of the distributed breach surface and actual pressure developed at this point is in order.



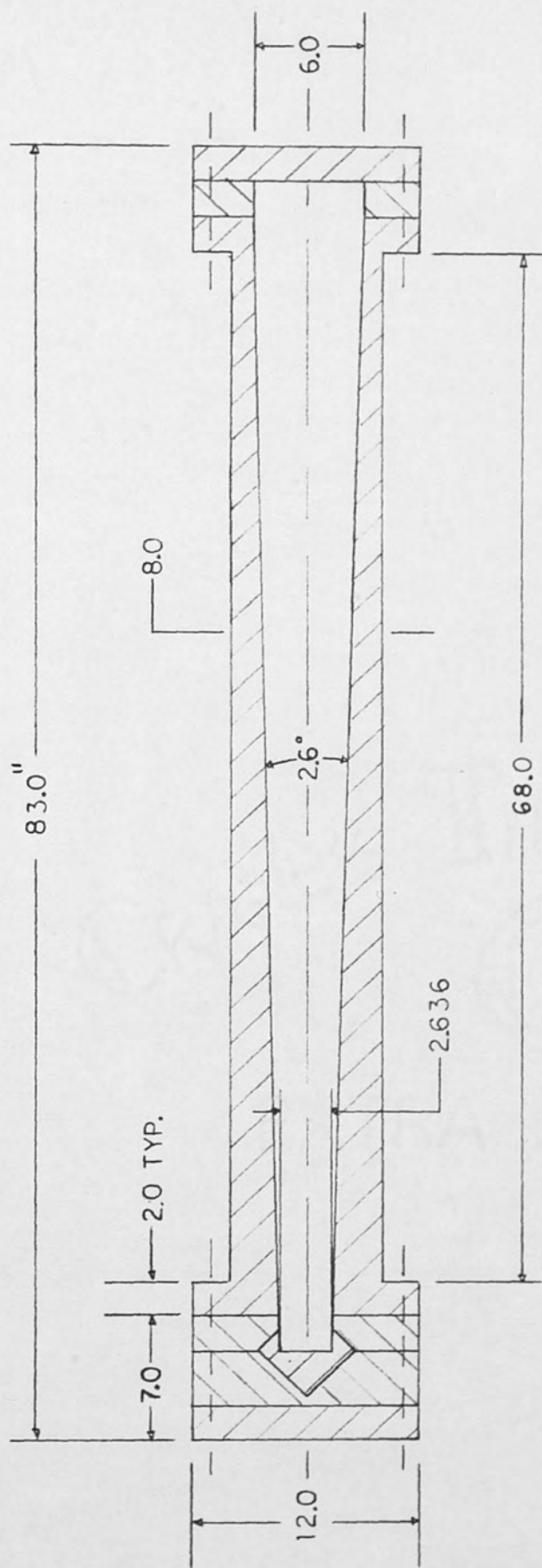


Fig. 2. Distributed breach shock tube

### III. DYNAMIC ANALYSIS

In order to predict the dynamic characteristics and response of the distributed breach shock tube design, a finite element computer model was developed by using SAP IV, a structural analysis program for the static and dynamic response of linear systems (Bathe, Wilson, and Peterson, 1974). This approach provides a powerful tool for the dynamic analysis of the tube and forms a basis for comparison of results obtained once the actual testing of the new design takes place in the future. Sanders (1981) reported excellent agreement between finite element predicted longitudinal natural frequencies and mode shapes and those estimated from frequency response data of the old shock tube. Unfortunately, only the longitudinal or axial dynamic characteristics of the tube were investigated with the finite element analysis. It seems logical, however, that a more in depth analysis using finite elements can provide a good approximation of other dynamic characteristics and ultimately the dynamic response of the new shock tube design.

The dynamic analysis has been carried out in two main parts: modal analysis and response history analysis.

In the modal analysis two different models are used to predict the tube's different natural frequencies and mode shapes. The response history analysis is used to predict displacements and stresses in the tube when subjected to the shock wave's loading characteristics.

Through these efforts, it is hoped that some insight can be gained into the behavior of the shock tube structure when exposed to the exotic loading conditions produced by the passing wave front.

#### Modal Analysis: Pipe Element Model

The SAP IV pipe element, shown in Figure 3, was used as a basis for the formulation of a possible finite element model of the shock tube primarily because all six degrees of freedom associated with the element's defining nodes have defined stiffness within the program. Thus, the member stiffness matrices account for bending, torsional, axial, and shearing deformations (Bathe, Wilson, and Peterson, 1974). The program forms the pipe element stiffness matrix by first evaluating the flexibility matrix at one end. Then, with the use of the corresponding stiffness matrix and some equilibrium transformations (curved beam stiffness coefficients), the complete element stiffness matrix is formulated.

The pipe element then seems to be ideally suited for the investigation of the shock tube's longitudinal, transverse, and rotational natural frequencies and mode



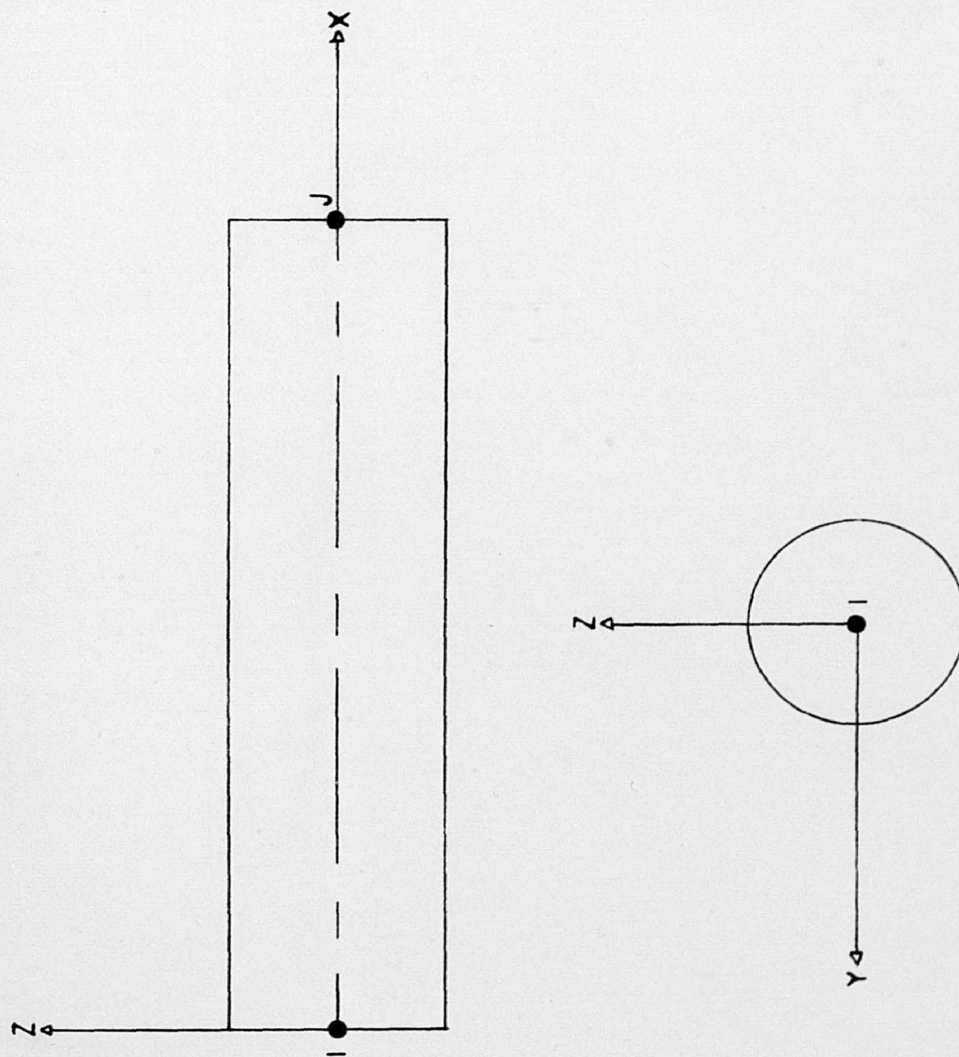


Fig. 3. SAP IV pipe element

shapes. These elements do, however, require a uniform section and uniform material properties. Therefore, in the conical region of the shock tube, the elements were incremented in wall thickness relative to the corresponding variation in inside diameter dictated by the geometry of the structure. Thus, in the 74.0 inch conical region, the elements were incremented accordingly from an inside diameter of 2.636 inches at the distributed breach (element 3) to an inside diameter of 5.909 inches at the muzzle end (element 25). The end plates and the steel backing jaws were also represented by pipe elements with an inside diameter of 0.0 inches, thus becoming solid disks. The complete structure and associated finite element layout is illustrated in Figure 4. A complete definition of the input data for the pipe element model is given in Chapter IV along with the associated output.

#### Modal Analysis: Axisymmetric Model

The SAP IV axisymmetric element, shown in Figure 5, was used to create a finite element model of the shock tube primarily to predict the radial natural frequencies and mode shapes. The element's defining nodes can only have two associate degrees of freedom which are, in our case, radial and longitudinal displacements. Thus, the axisymmetric model created can also be used to compare the longitudinal modal results obtained from the pipe element model.





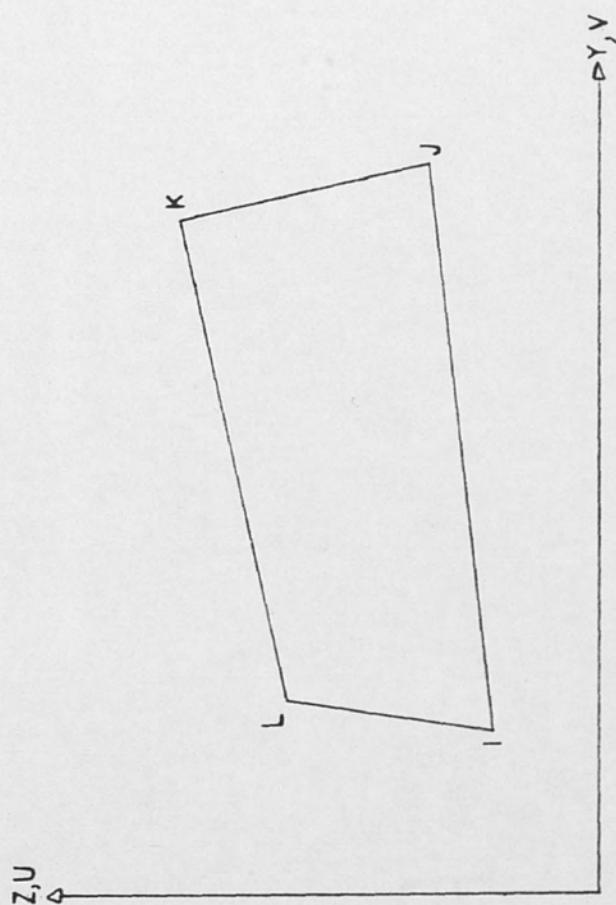


Fig. 5. SAP IV axisymmetric element

The axisymmetric element is based on an isoparametric formulation, and incompatible displacement modes can be included in order to improve the bending properties of the element (Bathe, Wilson, and Peterson, 1974). In addition, the element has temperature dependent orthotropic material properties. The way that the elements are defined makes it convenient to implement the exact tube geometry. Therefore, a very good idealization of the interior conical surface is realized. It is mentioned in the literature, however, that these elements reflect the greatest accuracy when they are rectangular in shape or, more specifically, a parallelogram. All of the tube elements input are rectangular with the exception of those bordering the interior conical surface. But, since the cone half angle is small at 1.3 degrees, the effect on the accuracy of these particular elements was assumed to be negligible.

The finite element axisymmetric model layout of the shock tube is shown in Figure 6. A complete description of the input data and the associated computer output is given in Chapter IV.

It is interesting to note at this point that in past investigations of the old shock tube structure, radial effects were not included or were thought to be insignificant at the lower resonances that were calculated. This may, indeed, be the case. However, the high frequency



content of the radial modal characteristics is of interest since the data noise obtained during past experiments is in the range above 25 kHz. It has been hypothesized in the past that this noise is structure borne or could be related to the circumferential modes of tube oscillation. Therefore, to help to give some insight into this phenomena, the radial modal characteristics of the new shock tube design have been investigated.

#### Response History Analysis

The response history analysis of the new design has been carried out in order to try and predict the dynamic response of the structure due to the time and magnitude varying load imposed by the shock wave as it propagates down the tube. With this analysis, stresses and displacements of the structure as a function of time can be calculated and the results compared to those obtained by Connell (1980), which assumed a static pressure to describe the elastic-plastic behavior of the tube.

The step-by-step integration method was employed in the SAP IV program. In this algorithm, the equations of motion are obtained by direct integration using the Wilson- $\theta$  method which is unconditionally stable (Bathe, Wilson, and Peterson, 1974). The Rayleigh form of damping is also assumed.

It is noted in the literature that this form of solution is ideal for shock problems because many modes



need to be included in the analysis and the response is required over relatively few time steps. The axisymmetric model developed earlier is again used for this analysis. This model was used primarily because in most practical analyses the use of isoparametric finite elements is the most effective (Bathe and Wilson, 1976).

A complete explanation of the input and associated computer output as well as a discussion of the obtained results is given in Chapter IV.

#### IV. SAP IV PROGRAM RESULTS

##### Modal Analysis: Pipe Element Model

This model was created using a total of 27 pipe elements with material properties corresponding to that of mild steel. Section properties were calculated and input according to the element's specific location along the tube axis. In each analysis it was necessary to fix node 1 completely so that rigid body motion of the model could not occur. Nodes 2 - 28 were given only one degree of freedom corresponding to the analysis mode in question. The results are shown below.

<u>Longitudinal (x) Natural Frequencies</u>		
<u>Mode</u>	<u>Frequency (cycles/sec)</u>	<u>Period (sec x 10<sup>-3</sup>)</u>
1	631.3	1.584
2	1716.0	0.5827
3	2961.0	0.3378
4	4202.0	0.2380
5	5337.0	0.1874
6	6403.0	0.1562
7	7546.0	0.1325
8	8752.0	0.1143
9	9957.0	0.1004
10	11,120.0	0.08989

Transverse (y) Natural Frequencies

<u>Mode</u>	<u>Frequency (cycles/sec)</u>	<u>Period (sec x 10<sup>-3</sup>)</u>
1	289.9	3.450
2	784.9	1.274
3	1360.0	0.7350
4	1947.0	0.5136
5	2504.0	0.3994
6	3007.0	0.3326
7	3493.0	0.2863
8	4010.0	0.2494
9	4542.0	0.2202
10	5067.0	0.1974

X-Rotational (θX) Natural Frequencies

<u>Mode</u>	<u>Frequency (cycles/sec)</u>	<u>Period (sec x 10<sup>-3</sup>)</u>
1	316.0	3.164
2	1026.0	0.9748
3	1874.0	0.5335
4	2707.0	0.3694
5	3387.0	0.2952
6	3955.0	0.2529
7	4695.0	0.2130
8	5497.0	0.1819
9	6287.0	0.1591
10	7044.0	0.1420

Y-Rotational ( $\theta_Y$ ) Natural Frequencies

<u>Mode</u>	<u>Frequency (cycles/sec)</u>	<u>Period (sec x <math>10^{-3}</math>)</u>
1	4748.0	0.2106
2	5996.0	0.1668
3	6477.0	0.1544
4	6995.0	0.1430
5	7470.0	0.1339
6	7992.0	0.1251
7	8737.0	0.1145
8	9579.0	0.1044
9	10,450.0	0.09567
10	11,320.0	0.08831

The associated mode shapes for the first 3 modes of each case are shown in Figures 7 - 14.

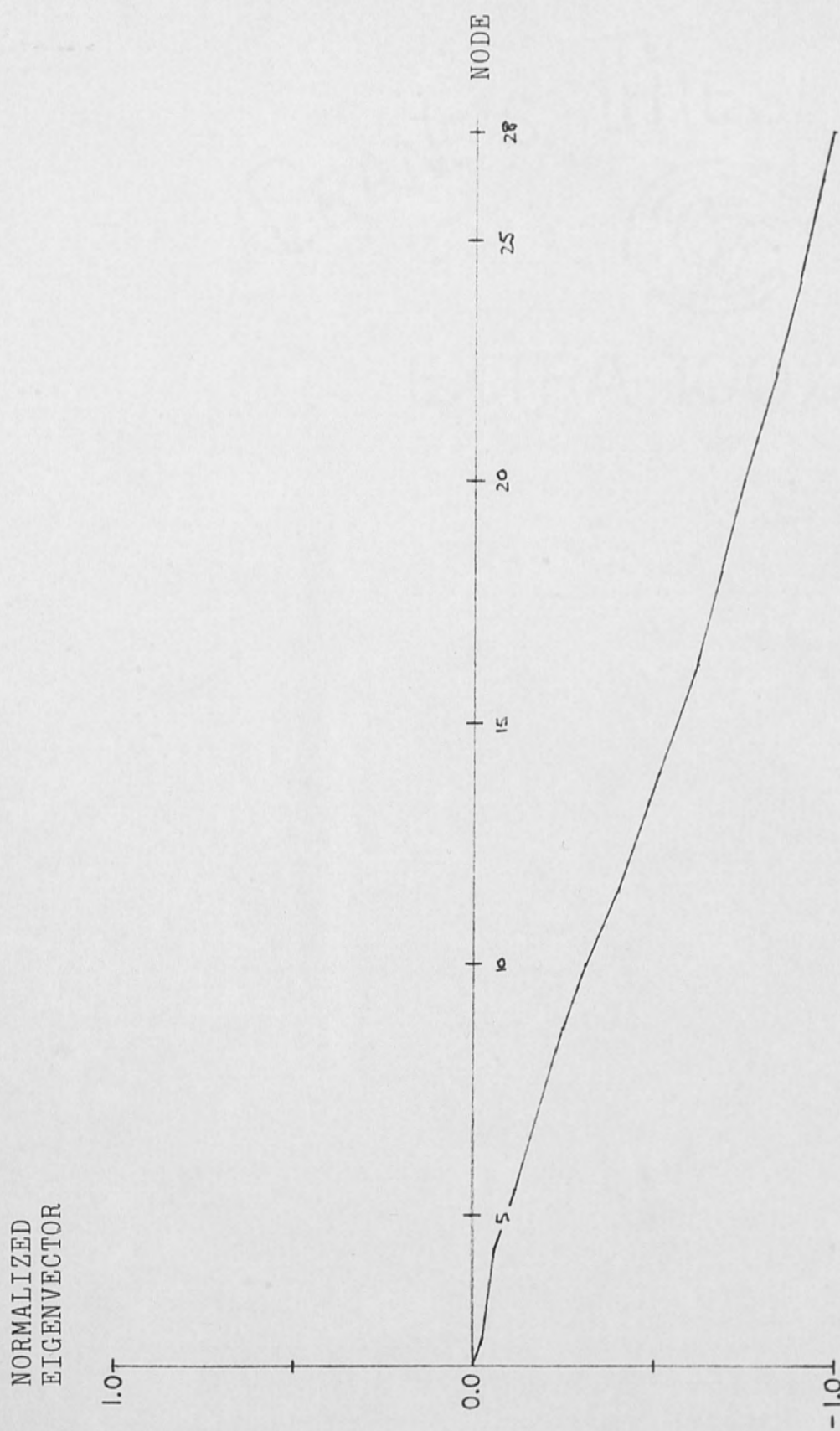


Fig. 7. First longitudinal mode shape



NORMALIZED  
EIGENVECTOR

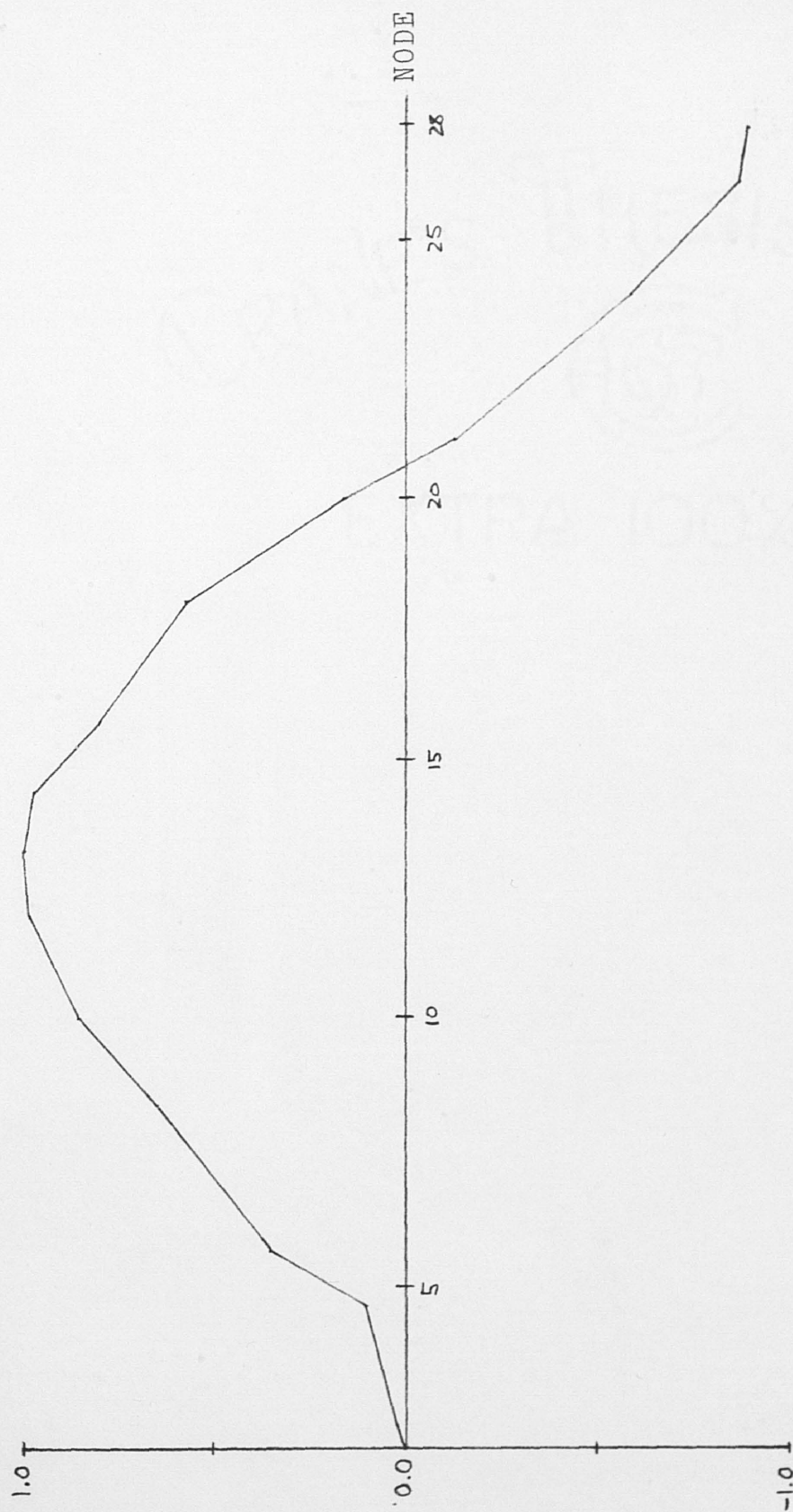


Fig. 8. Second longitudinal mode shape

NORMALIZED  
EIGENVECTOR

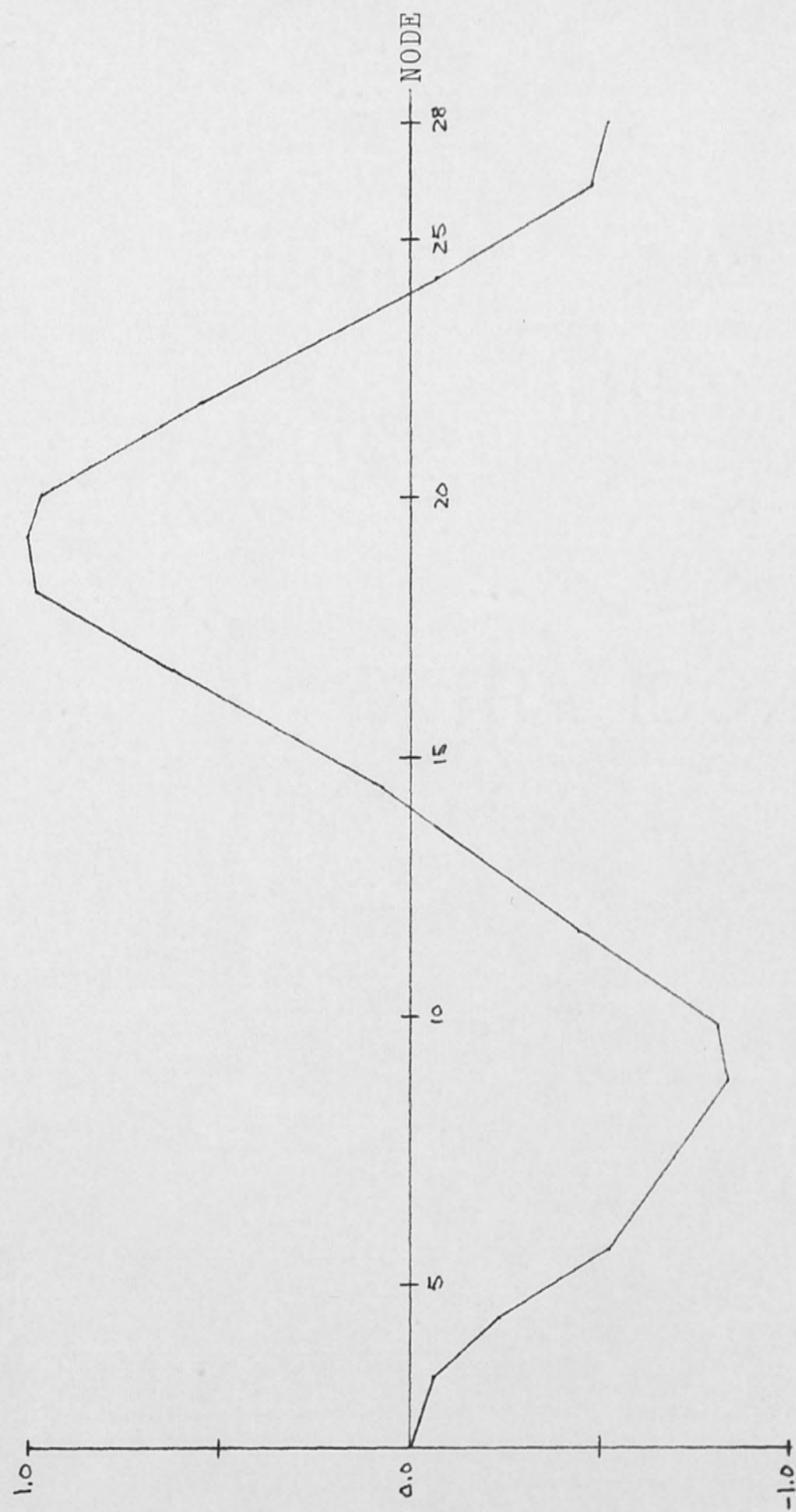


Fig. 9. Third longitudinal mode shape

NORMALIZED  
EIGENVECTOR

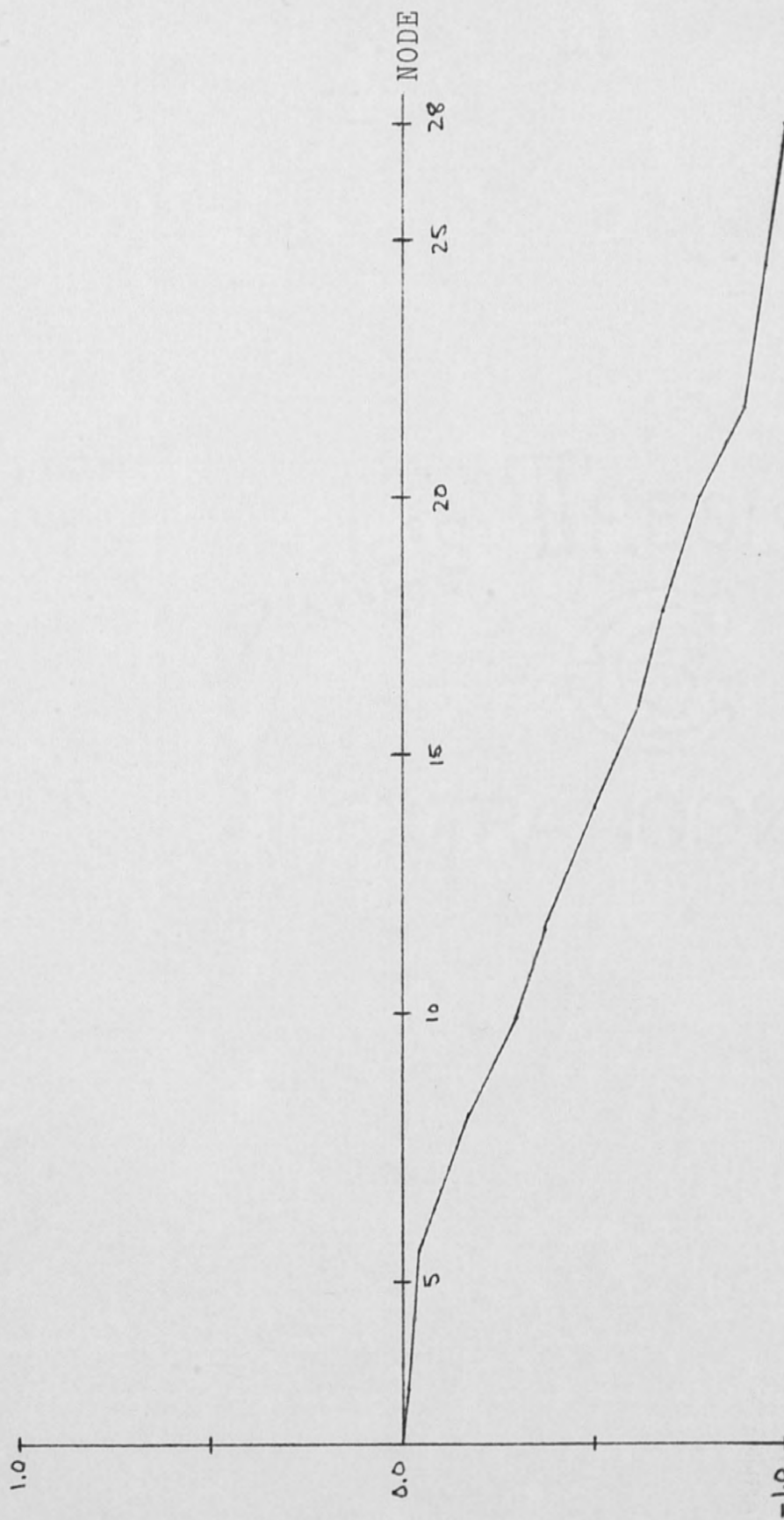


Fig. 10. First transverse mode shape

NORMALIZED  
EIGENVECTOR

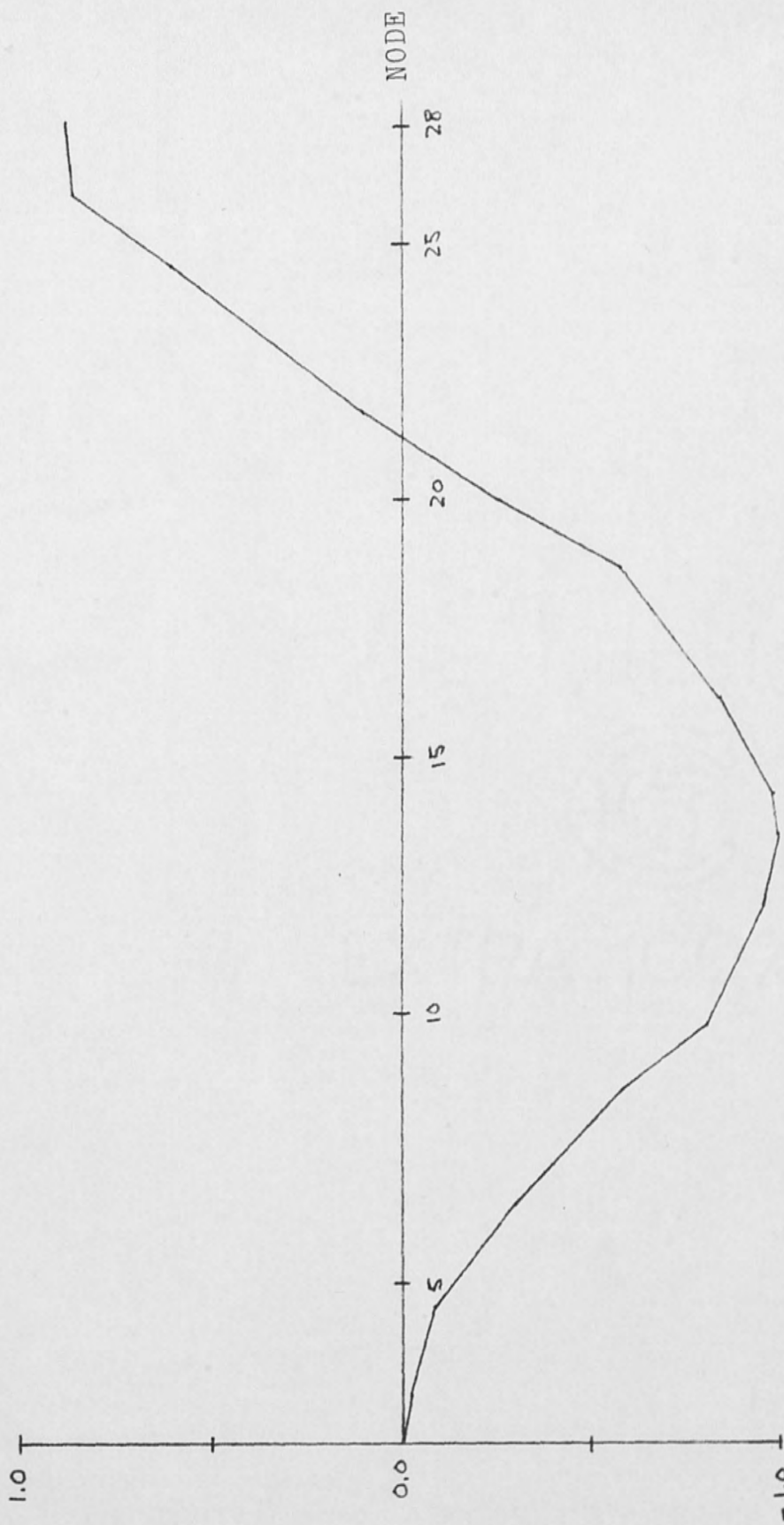


Fig. 11. Second transverse mode shape



NORMALIZED  
EIGENVECTOR

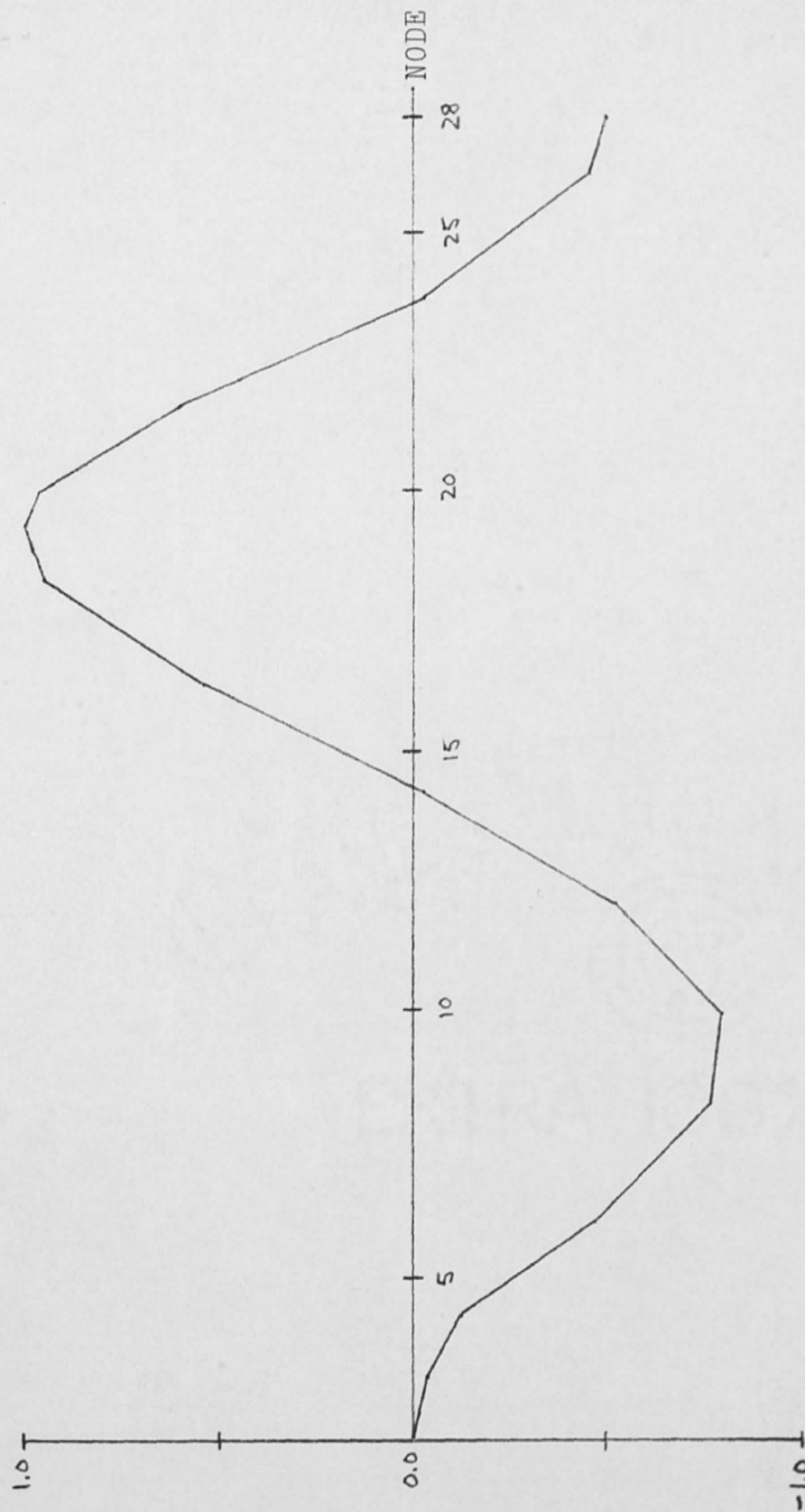


Fig. 12. Third transverse mode shape



NORMALIZED  
EIGENVECTOR

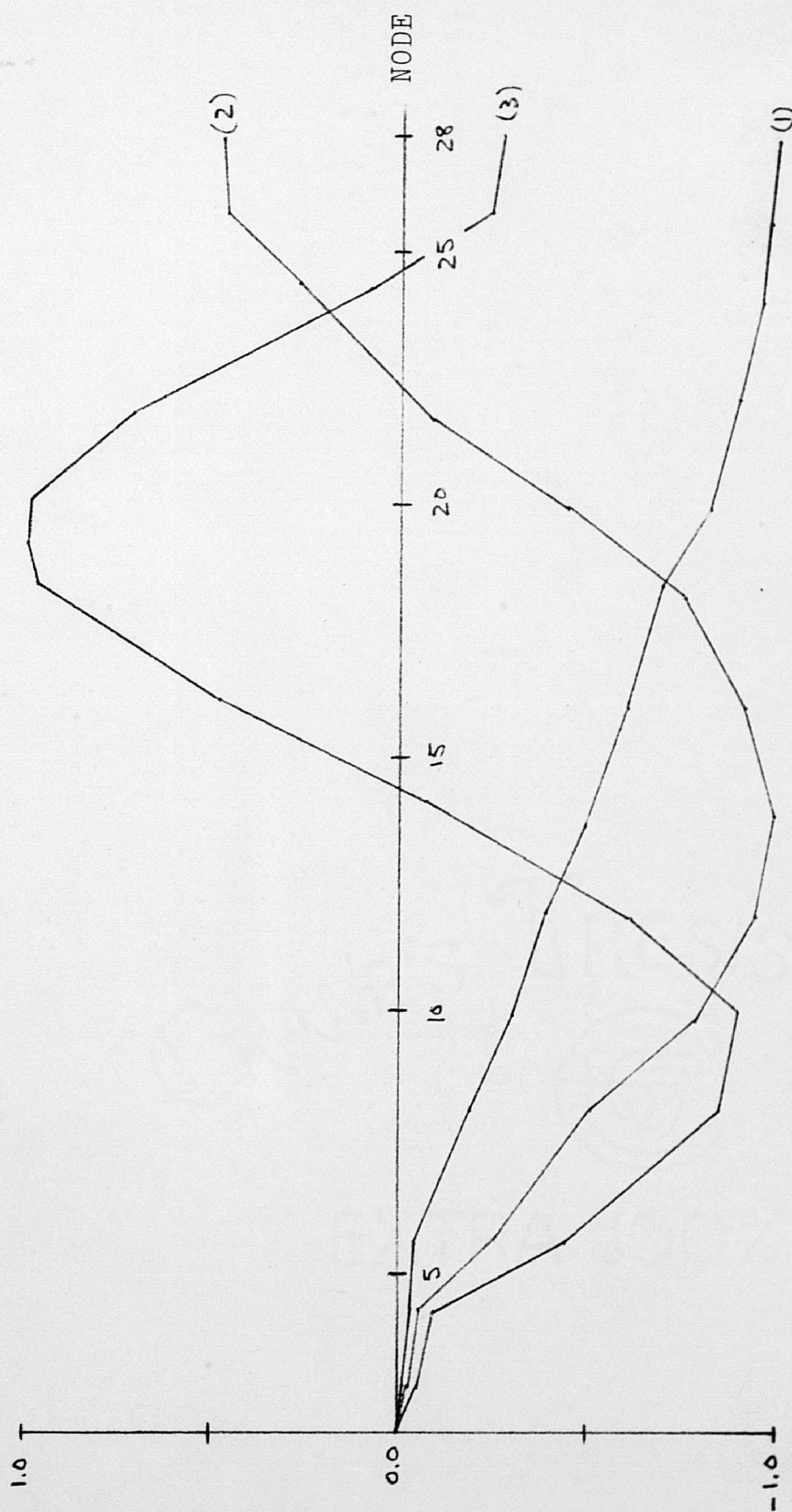


Fig. 13. X-rotational mode shapes

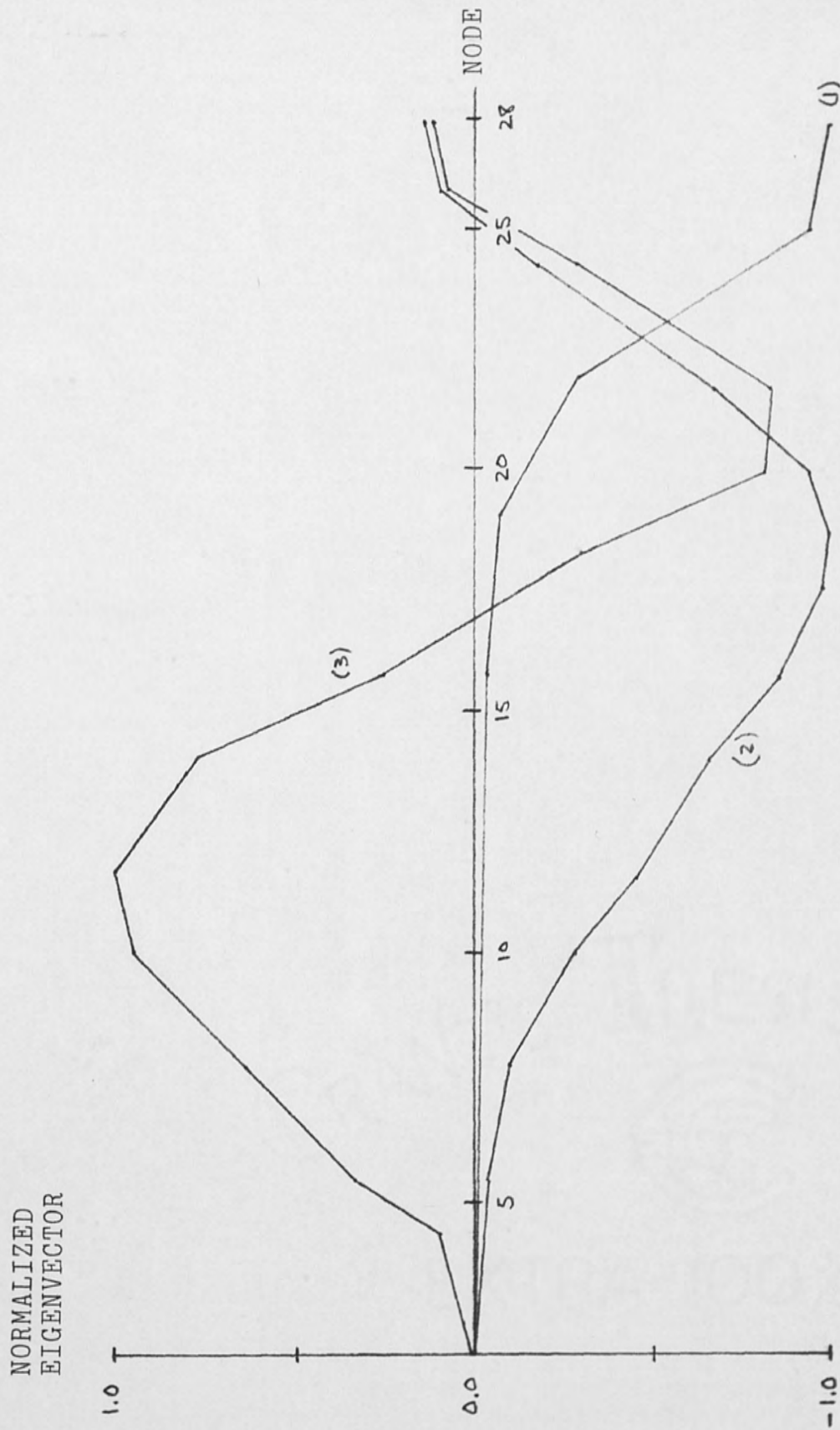


Fig. 14. Y-rotational mode shapes

### Modal Analysis: Axisymmetric Model

The axisymmetric shock tube model was created by using a total of 33 rectangular and nearly rectangular elements to represent the structure. These elements have symmetry about the longitudinal (Z) axis and thus are defined in the Y-Z plane (see Fig. 6). The nodal points which lie on the interior conical surface were incremental in the radial (Y) direction as a function of tube geometry and axial position along the tube axis. Elements at the breach and muzzle ends were given dimensions that closely resemble the actual tube dimensions at these points. The results of the radial and longitudinal modal analysis using this model are shown below.

#### Radial (Y) Natural Frequencies

<u>Mode</u>	<u>Frequency (cycles/sec x 10<sup>3</sup>)</u>	<u>Period (sec x 10<sup>-5</sup>)</u>
1	12.58	7.947
2	12.82	7.799
3	14.58	6.860
4	15.56	6.426
5	16.07	6.221
6	16.17	6.183
7	17.17	5.826
8	18.30	5.464
9	19.10	5.237
10	19.13	5.228

Longitudinal (Z) Natural Frequencies

<u>Mode</u>	<u>Frequency (cycles/sec)</u>	<u>Period (sec x 10<sup>-3</sup>)</u>
1	685.9	1.458
2	1848.0	0.5411
3	3187.0	0.3138
4	4532.0	0.2207
5	5770.0	0.1733
6	6887.0	0.1452
7	8031.0	0.1245
8	9233.0	0.1083
9	10,410.0	0.09608
10	11,140.0	0.08980

From these results, two interesting conclusions can be drawn. First, note the high frequency content of the radial natural frequencies. This could be one source of explanation for the data scatter and noise obtained in previous tests with the old tube. Filler (1964) has also mentioned this phenomena as a possible explanation for the scatter of data between actual and predicted results.

We can also see that the longitudinal frequencies predicted by the axisymmetric and pipe finite element models are in good agreement. Thus, the longitudinal vibrational characteristics of the tube have been verified by using two different models.

### Response History Analysis

Using the empirical scaling laws as a basis for loading characteristics, the dynamic response of the previously developed axisymmetric model was predicted. Each node on the interior conical surface was subjected to a different forcing function, conservatively estimated by a discontinuous peak followed by a linear decay for simplicity. This concept is illustrated in Figure 15. This curve also fits relatively well to the data obtained by Rogers (1977) and Poche' (1971).

Two function definition points were required, and these correspond to the characteristics obtained from the scaling laws. Thus, at each interior node a different forcing function was defined with different wave characteristics as governed by the scaling laws. Independent arrival times were also specified for each forcing function corresponding to the arrival time of the shock wave as it propagates down the tube. Based on a propagation speed of about 5000 ft/sec in water, we see that the wave propagates the entire tube length in 1267 microseconds. At this same range, it takes 3122 microseconds for the pressure to fall from a peak



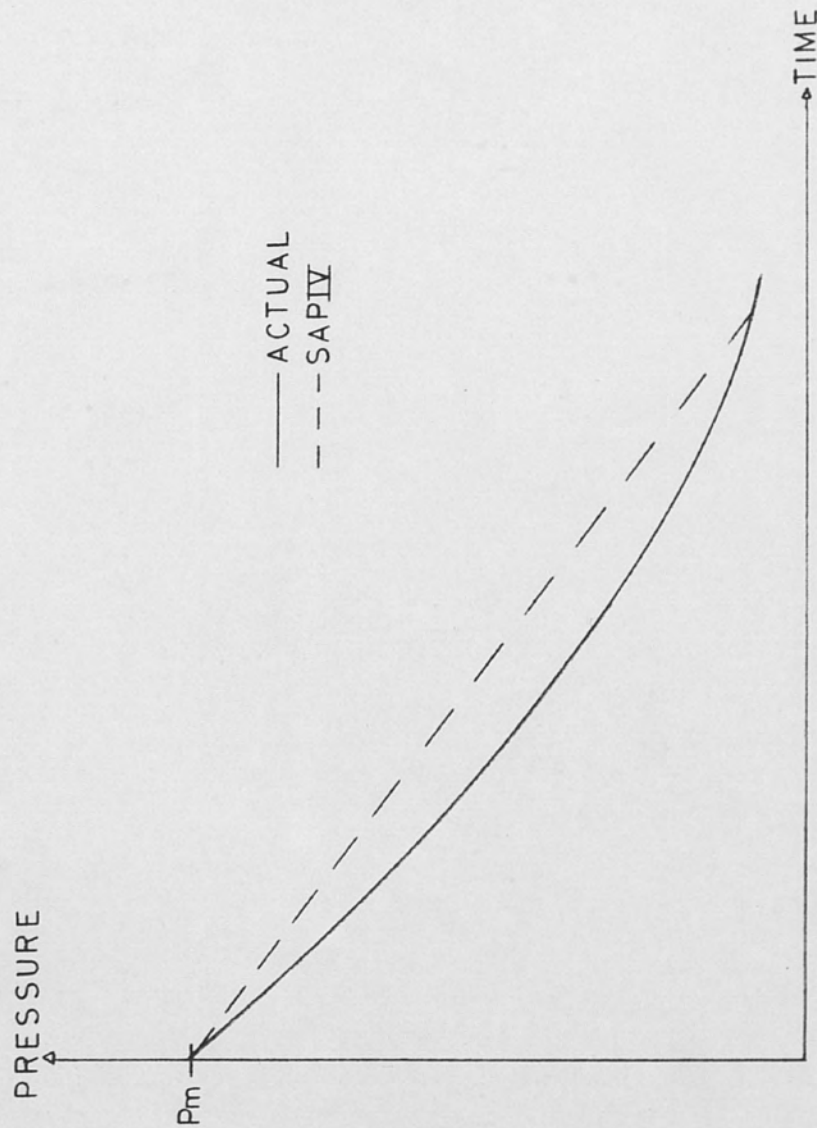


Fig. 15. Actual waveform and SAP IV Input

value of 9213 psi to 1 psi. In contrast, at the distributed breach it takes 2843 microseconds for the pressure to fall from 25,647 psi to 1 psi. Thus, the total solution time was chosen to be  $\tau = 2800$  microseconds with a time step  $\Delta t = 4$  microseconds for a total of 700 solution time steps. Note that this choice of  $\Delta t$  also satisfies the requirement that

$$\frac{\Delta t}{T} < 0.1$$

where  $T$  = the period of the highest numbered mode that is to be included in the response calculation (Bathe, Wilson, and Peterson, 1974). In our case,  $T = 0.5228 \times 10^{-4}$  seconds.

The maximum displacements developed at some of the nodes are shown below.

<u>Node</u>	<u>Maximum Displacement (in)</u>	<u>Direction</u>
11	-0.02977	Z
13	0.003661	Y
13	0.0051247	Z
16	0.007601	Y
16	0.0082333	Z
19	0.0093189	Y
19	0.012339	Z
22	0.0072669	Y
22	0.02156	Z
34	0.0070758	Y
34	0.08033	Z
50	0.0026768	Y
50	0.17276	Z
52	0.01191	Y
52	0.18049	Z
55	0.0064555	Y
55	0.18318	Z
58	0.25384	Z
60	-0.0032672	Y
60	0.19515	Z

The stresses developed at the center of some of the elements are shown below. The convention for the output stresses is shown in Figure 16. From the figure, we see that  $v$  and  $u$  are the normal stresses, with  $uv$  being the shear stress developed at the element center. The symbol  $T$  represents the third principle stress which acts on the plane of the element.

Maximum Stress Components at Center (ksi)

<u>Element</u>	<u>v</u>	<u>u</u>	<u>T</u>	<u>uv</u>
7	-35.96	43.01	29.44	20.13
9	-53.09	55.10	38.92	11.80
11	-41.78	96.73	41.72	-12.34
17	-68.27	87.61	32.41	-10.20
26	-47.35	87.39	58.32	15.48
27	-56.58	39.96	57.34	-15.30
4	37.96	-126.6	53.12	126.1
5	-19.06	24.18	10.47	13.52
32	-30.37	28.63	36.01	15.72
31	41.95	-85.57	48.60	-111.90
29	-34.12	59.45	23.79	-22.04

A discussion of the obtained results is now in order. First, note that radial ( $y$ ) displacements at all of the output nodes seem to be small. The larger values of longitudinal ( $z$ ) displacements along the interior conical surface (nodes 50, 52, and 55) are most likely due to the fact that the horizontal components of the forces developed

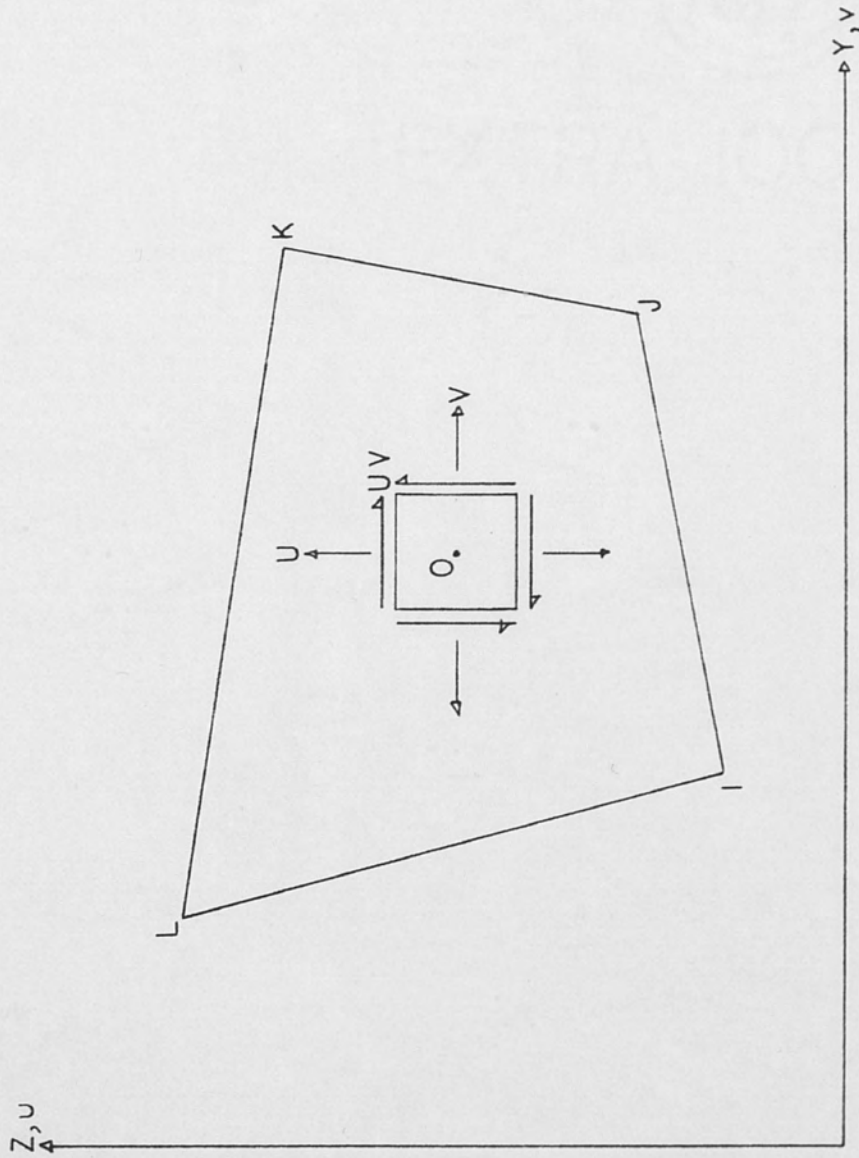


Fig. 16. Output stress convention



at these nodes were neglected in the analysis. It can also be seen that a relatively large longitudinal maximum displacement occurs at node 58, the center of the muzzle end plug.

The radial stresses developed are slightly higher than those predicted in the static analysis of the old shock tube (Connell, 1980). The largest radial stress is seen to occur near the middle of the tube (element 17). The largest longitudinal stress component occurs, as expected, at the breach plug (element 4). Longitudinal stress as a function of time is shown in Figure 17 for element 4. The radial stress time function for element 17 is presented in Figure 18.



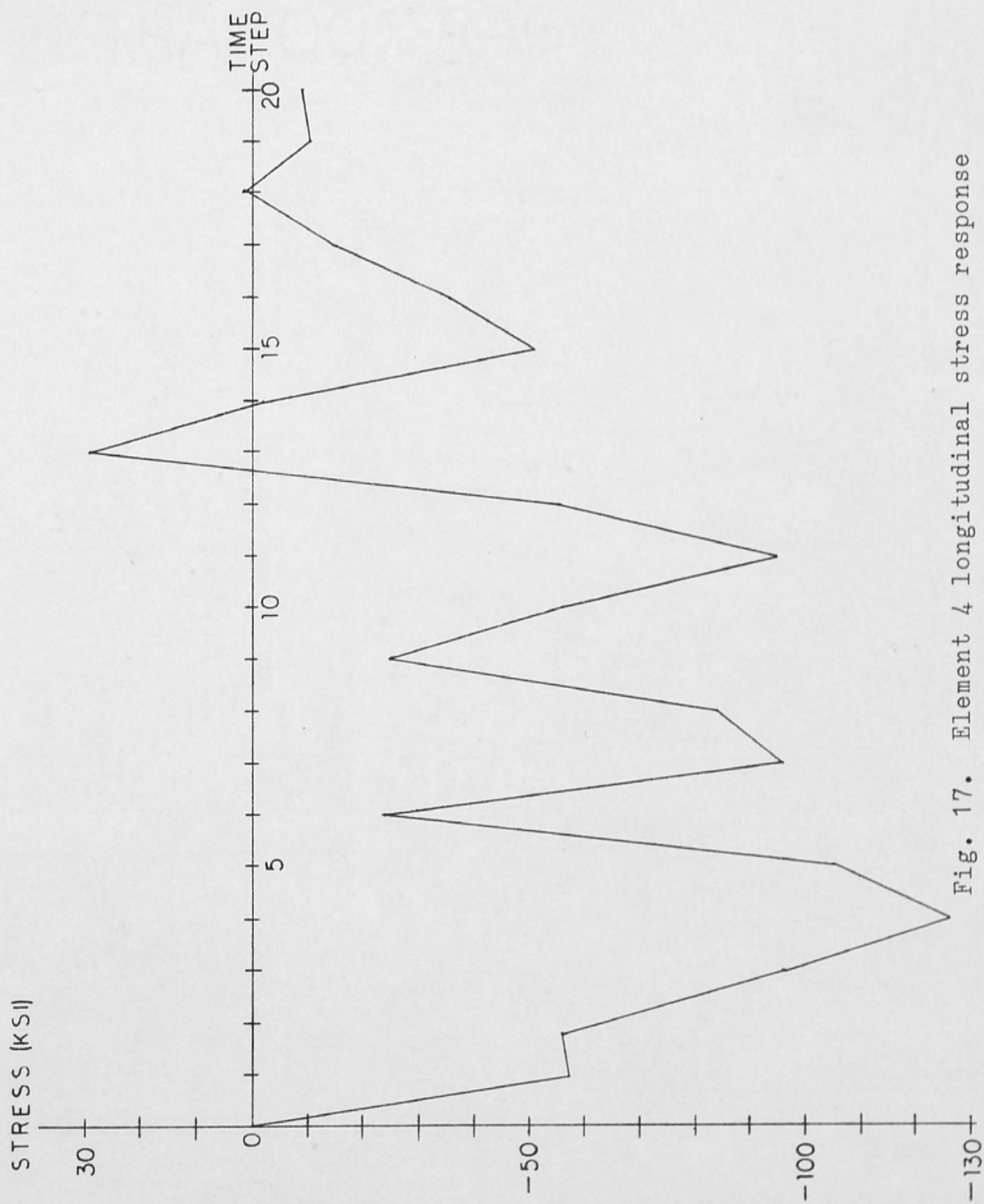


Fig. 17. Element 4 longitudinal stress response

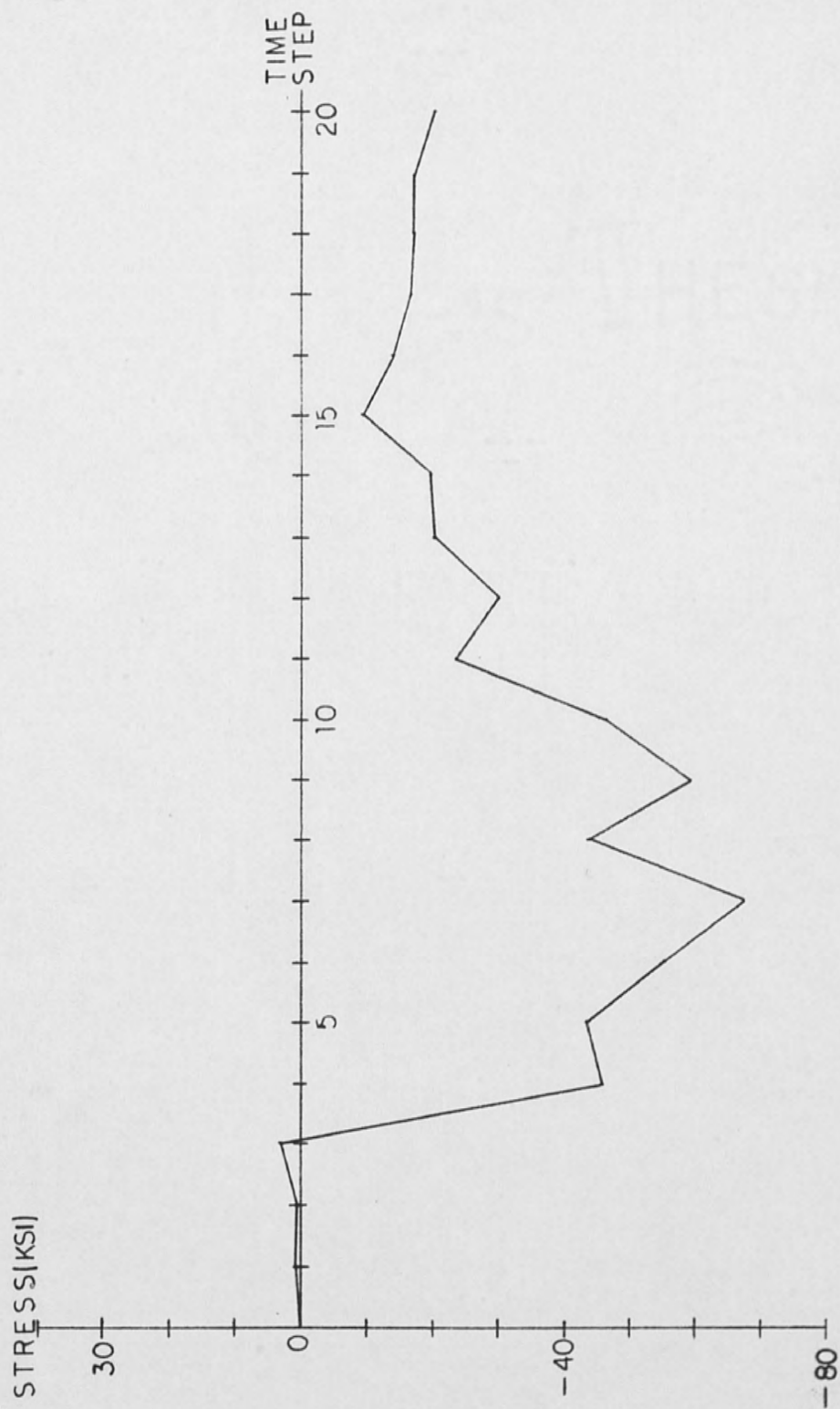


Fig. 18. Element 17 radial stress response

## CONCLUSION

With the use of the SAP IV structural analysis program, a comprehensive dynamic analysis of the distributed breach conical shock tube has been performed. Natural frequencies and mode shapes have been calculated, with the results being in the generally expected range. A dynamic stress analysis has also been carried out which shows the fluctuating nature of the element stresses as the shock wave propagates along the tube axis. Maximum stresses obtained have higher values than those obtained in previous analyses of the old structure. This fact alone justifies the need for a dynamic analysis of this type of loading and structure. It is true that these high stresses are not applied for much of a time duration, thus immediate failure of the tube structure is not likely. However, over a period of time as many shots are made and internal pressures approach ideal values, a cyclic loading of the tube is recognized and a comprehensive fatigue failure analysis becomes desirable. With the use of nondestructive testing techniques and fracture mechanics research, a fascinating area of study can be applied to a relatively complex structure.

It is hoped that the effort put forth in this paper can be utilized in future research into the failure analysis of the shock tube.

## REFERENCES

- Arons, A. B. "Underwater Explosion Shock Wave Parameters at Large Distances from the Charge." J. Acoust. Soc. Am. 26 (May 1954): 343-46.
- Bathe, K. J., Oden, J. T., and Wunderlich, W. Formulations and Computational Algorithms in Finite Element Analysis. U.S.-Germany Symposium, 1976.
- Bathe, K. J., and Wilson, E. L. Numerical Methods in Finite Element Analysis. Englewood Cliffs, New Jersey: Prentice-Hall, 1976.
- Bathe, K. J., Wilson, E. L., and Peterson, F. E. SAP IV: A Structural Analysis Program for Static and Dynamic Response of Linear Systems. Virginia: National Technical Information Service, 1974.
- Connell, L. W. "Design and Analysis of an Explosion Driven Hydrodynamic Conical Shock Tube." Masters Research Report, University of Central Florida, 1980.
- Den Hartog, J. P. Advanced Strength of Materials. New York: McGraw-Hill, 1952.
- Filler, W. S. "Propagation of Shock Waves in a Hydrodynamic Conical Shock Tube." Physics of Fluids 7 (May 1964): 664-67.
- Moslehy, F. A., and Metwalli, S. M. "Design and Testing of Distributed Breach for the Conical Shock Tube and Investigating Ringing Abatement Methods." Proposal to the Naval Research Laboratory, University of Central Florida, 1982.
- Poche, L. B. "Underwater Shock-Wave Pressures from Small Detonators." J. Acoust. Soc. Am. 51 (October 1971): 1733-37.
- Popov, E.P. Introduction to Mechanics of Solids. Englewood Cliffs, New Jersey: Prentice-Hall, 1968.



- Rogers, P. H. "Weak-Shock Solution for Underwater Explosive Shock Waves." J. Acoust. Soc. Am. 62 (December 1977): 1412-19.
- Saada, A. S. Elasticity: Theory and Applications. New York: Pergamon Press, 1974.
- Sanders, W. R. "Analysis of Structural Dynamic Characteristics of an Explosion Driven Hydrodynamic Conical Shock Tube." Masters Research Report, University of Central Florida, 1981.
- Shigley, J. E. Mechanical Engineering Design. New York: McGraw-Hill, 1963.
- Timoshenko, S. P., and Gere, J. M. Mechanics of Materials. New York: D. Van Nostrand Company, 1972.
- Venkatraman, B., and Patel, S. A. Structural Mechanics with Introductions to Elasticity and Plasticity. New York: McGraw-Hill, 1970.